tion causes mass flow in the wetted wick, that, in turn distorts the shape of the meniscus. This effect should be of second-order nature but is difficult to estimate quantitatively. Evaporation also introduces a dynamic pressure difference across the liquid–vapor interface, but this difference can be shown to be always negligible as compared to the static pressure difference. This is further confirmed by the successful correlation of the data of Freon 11, which were obtained under intense evaporation conditions at room temperature. Another possible effect is that of the contact angle. That this effect is negligible as implied in the present correlation can be explained through the physical model for screen wicks shown in Fig. 1. Each meniscus is tangent to its adjacent ones at the instant of rupture. The surface tension force at the tangent point acts vertically upward and is balanced by the downward pull of the liquid column. This model is analogous to that of the ring method for surface tension measurements [12], in which the dependence on contact angle was found to be indeed small [12, 13].

REFERENCES

1. H. R. KUNZ, L. S. LANGSTON, B. H. HILTON, S. S. WYDE and G. H. NASHICK, Vapor chamber fin studies, Transport properties and boiling characteristics, NASA CR-812 (1967). Also, L. S. LANGSTON and H. R. KUNZ, Liquid transport properties of some heat pipe wicking materials, ASME Paper No. 69-HT-17 (1969).
2. S. KATZOFF, Heat pipe and vapor chambers for thermal control of spacecraft, *Thermophysics of Spacecraft and Planetary Bodies*, pp. 761–818. Academic Press (1967).
3. E. SCHMIDT, Contribution a l'etude des calodues, Ph.D. thesis, University of Grenoble, France (1968).
4. J. K. FERRELL and J. ALLEAVITCH, Vaporization heat transfer in capillary wick structure, A.I.Ch.E. Preprint No. 6, *ASME–AIChE Heat Transfer Conference*, Minneapolis, Minnesota (August 1969).
5. E. C. PHILLIPS and J. D. HINDERMAN, Determination of properties of capillary media useful in heat pipe design, ASME Paper No. 69-HT-18 (1969).
6. J. BOHDANSKY, H. STRUB and E. VAN ANDEL, Heat transfer measurements using a sodium heat pipe working at low vapor pressure, *Proceedings of Thermionic Conversion Specialist Conference*, Houston, Texas, pp. 144–148 (November 1966).
7. A. E. SCHEIDEGGER, *The Physics of Flows Through Porous Media*, pp. 3–18, 115–117. Macmillan, New York (1960).
8. D. M. ERNST, Evaluation of theoretical heat pipe performance, *Proceedings of Thermionic Conversion Specialist Conference*, pp. 349–354 (October 1967).
9. J. E. KEMME, Ultimate heat pipe performance, *IEEE Trans. Electron Devices* **ED-16**, No. 8 (August 1969).
10. D. M. ERNST, E. K. LEVY and P. K. SHEFSIEK, Heat pipe studies at thermo electron corporation, *Thermionic Conversion Specialist Conference*, pp. 254–257 (October 1968).
11. A. V. LUIKOV, *Heat and Mass Transfer in Capillary Porous Bodies*, 1st edn., pp. 205–220. Pergamon Press, NewYork (1966).
12. J. R. PARTINGTON, *An Advanced Treatise on Physical Chemistry*, Vol. II, pp. 117–118. Longmans, London (1951).
13. J. T. DAVIES and E. K. RIDEAL, *Interfacial Phenomena*, pp. 42–44. Academic Press, New York (1961).

Int. J. Heat Mass Transfer. Vol. 14, pp. 1855–1859. Pergamon Press 1971. Printed in Great Britain

COMPRESSIBLE GAS FLOW THROUGH A POROUS MATERIAL

G. S. BEAVERS and E. M. SPARROW

School of Mechanical and Aerospace Engineering, University of Minnesota, Minneapolis, Minnesota, U.S.A.

(*Received* 8 *May* 1970 *and in revised form* 13 *January* 1971)

NOMENCLATURE

a, sound speed;
A, total cross-sectional area normal to the streamwise direction;
A_p, cross-sectional area of pore space normal to the streamwise direction;
c, constant related to losses due to separation and turbulence;
k, permeability;
L, length of porous material;
L_{max} length of porous material required for choking;
M, Mach number, u/a;

$\dot{m}$, mass flow rate;
p, static pressure;
R, irreversible flow resistance;
Re, Reynolds number, $\rho V\sqrt{k}/\mu$;
T, absolute temperature;
u, mean pore velocity;
V, mean filter velocity (Darcy velocity);
x, streamwise coordinate.

Greek symbols
γ, ratio of specific heats;
ε, porosity;
μ, viscosity;
ρ, density.

INTRODUCTION

THERE exists an extensive literature on the flow of fluids through porous materials, most of which is concerned with incompressible, inertia-free flows (e.g. [1, 2]). Little attention has been given to compressible gas flows through porous materials at velocities which are sufficiently high to cause significant effects of inertia. An important contribution to this problem area has been made by Emanuel and Jones [3], who developed a one-dimensional theory for compressible adiabatic flow of a perfect gas through a porous medium. The objective of the present work is to extend and generalize the analysis of the problem treated by Emanuel and Jones.

A schematic diagram of the physical system is given in the inset of Fig. 1. Stations 1 and 4 correspond, respectively, to locations immediately upstream and downstream of the porous material. Station 2 lies within the porous material, just downstream of the front face, and between 1 and 2 the flow adjusts to accommodate the change in the open cross-sectional area. Similarly, station 3 is situated just within the porous material, at its downstream end. The distance between stations 1 and 2 and between stations 3 and 4 will usually be of the order of a few pore diameters and will thus be negligible compared with the overall length of the material. Consequently, distances in the streamwise direction can be measured without ambiguity from the front face of the material. The foregoing notation is the same as that of [3]. The porous material is taken to be homogeneous and isotropic.

FLOW WITHIN THE POROUS MATERIAL

The flow within the porous material between stations 2 and 3 is now considered. For a one-dimensional model, the relevant conservation equations may be written as

$$\rho u\, \mathrm{d}u/\mathrm{d}x = -\mathrm{d}p/\mathrm{d}x - R \tag{1}$$

$$C_p \mathrm{d}T + u\mathrm{d}u = 0 \tag{2}$$

$$\mathrm{d}(\rho u) = 0. \tag{3}$$

The quantity u is the mean fluid velocity through the pore space at any cross section and is given by

$$u = \dot{m}/\rho A_p \tag{4}$$

where A_p the cross-sectional area of the pore space, is assumed to be independent of the axial coordinate x. The resistance R appearing in equation (1) characterizes the irreversibilities experienced by the flow as it passes through the porous material (i.e. the flow is not isentropic). The energy equation (2) corresponds to negligible heat transfer at the outer bounding walls of the porous material.

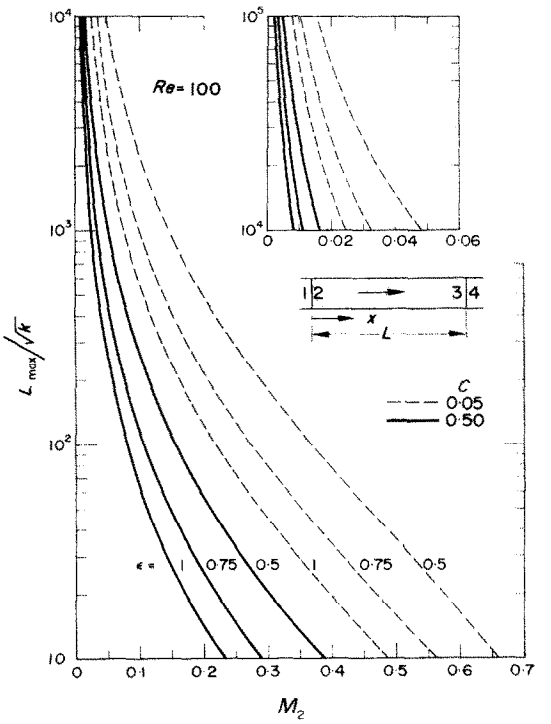

FIG. 1. Axial length of porous material for choking, $Re = 100$.

To proceed, it is necessary to specify the resistance R. Recent experiments [4–6] involving liquid flows in porous materials have shown that R can be very well described by

$$R = \varphi\mu V/k + c\rho V^2/\sqrt{k}. \tag{5}$$

Here, V is a superficial velocity (Darcy velocity) defined by

$$V = \dot{m}/\rho A \tag{6}$$

in which A is the total cross-sectional area normal to the flow. Although equation (5) was deduced from incompressible flow experiments, there is ample precedent ([7], p. 184) to support its application to subsonic compressible

flows. In equation (5), k is the permeability and c is a constant that depends on the particular class of porous materials under consideration. The first term appearing on the right-hand side represents the viscous resistance (Darcy resistance) characterizing a laminar inertia-free flow. The second term on the right takes account of losses due to separation and turbulence.

For a porous material in which the pore space is isotropically and randomly distributed, the fractional pore volume in any layer of infinitesimal thickness dx is equal to the fractional pore area [1], i.e. $\varepsilon = A_p/A$, where ε is the porosity. Then, if the density ρ which occurs in the defining equation (6) for the Darcy velocity is taken to be the local gas density as it appears in equations (1), (3) and (4), it follows at once that

$$V = \varepsilon u. \tag{7}$$

The substitution of equations (7) and (5) into equation (1) yields

$$\rho u \frac{du}{dx} = -\frac{dp}{dx} - \left(\frac{\varepsilon\mu}{k}u + \frac{\varepsilon^2 c}{\sqrt{k}}\rho u^2\right) \tag{8}$$

which, aside from the quadratic resistance term, has the same form as the momentum equation of Wankat and Schowalter [8]. In connection with equation (8), it is relevant to note that, for porous materials, small ε usually implies small k.

Then, equation (8) may be recast into dimensionless form, with the result

$$\gamma M^2 \frac{du}{u} + \frac{dp}{p} + \gamma M^2 \varepsilon^2 \left(\frac{dx}{\sqrt{k}}\right)\left(\frac{1}{Re} + c\right) = 0 \tag{9}$$

where

$$Re = \frac{\rho u \varepsilon \sqrt{k}}{\mu} = \frac{\rho V \sqrt{k}}{\mu}; \quad M = \frac{u}{a}. \tag{10}$$

The Reynolds number defined by equation (10) has been previously employed in correlating incompressible pressure drop data for porous media [4–6]. It is appropriate to discuss the components $1/Re$ and c which make up the dimensionless form of the resistance law $(1/Re + c)$ appearing in equation (9). Only when $1/Re \gg c$ are the irreversibilities limited to the viscous losses of a Darcy flow. Otherwise, both components of the resistance law must be accounted for. Thus far, c values varying from approximately 0·075 to 0·5 have been measured [4–6]. Therefore, in some cases, significant departures ($\geqslant 2$ per cent) from the Darcy resistance occur at Reynolds numbers as low as 0·04.

Next, by making use of equations (2) and (3) in conjunction with the perfect gas law, equation (9) can be reduced to a differential equation relating the Mach number M and the dimensionless axial position $x/\sqrt{k}$. Upon integration from $x = 0$, where the Mach number is M_2, to any axial station $x/\sqrt{k}$ with Mach number M, there is obtained

$$2\varepsilon^2(1/Re + c)x/\sqrt{k} = F(M_2^2) - F(M^2) \tag{11}$$

where

$$F(M^2) = \frac{1}{\gamma M^2} + \left(\frac{\gamma+1}{2\gamma}\right)\ln\left[\frac{M^2}{1 + (\gamma-1)M^2/2}\right]. \tag{12}$$

Equation (11) may be employed to specify the axial length L_{max} of porous material required to produce choking of the flow at station 3 (i.e. $M_3 = 1$). The result is

$$\frac{L_{max}}{\sqrt{k}} = \frac{1}{2\varepsilon^2}\left(\frac{1}{Re} + c\right)^{-1} G(M_2^2) \tag{13}$$

where

$$G(M_2^2) = \frac{1 - M_2^2}{\gamma M_2^2} + \left(\frac{\gamma+1}{2\gamma}\right)\ln\left[\frac{(\gamma+1)M_2^2}{2(1 + (\gamma-1)M_2^2/2)}\right]. \tag{14}$$

It will be observed that $G(M_2^2)$ is numerically equal to the function $4\bar{f}L_{max}/D$ for adiabatic flow with friction in a constant area duct [7]. As prescribable parameters, equations (11) and (13) contain the material constants k, ε and c, the specific heat ratio γ, the Reynolds number Re, and the initial Mach number M_2.

To illustrate the nature of the results, Figs. 1–3 present $L_{max}/\sqrt{k}$ as a function of M_2 for Reynolds numbers of 100, 1·0 and 0·1 respectively ($\gamma = 1{\cdot}4$). Each figure contains curves for ε values of 0·5, 0·75 and 1·0 with two values of c (0·5 and 0·05) used at each ε. The presentation is limited to $L_{max}/\sqrt{k} \geqslant 10$, this limit being selected both from the standpoint of practicality of fabrication and to insure the validity of the analytical model.

When the flow Reynolds number is as high as 100, the viscous (Darcy) resistance ($\sim 1/Re$) is completely overwhelmed by the inertial resistance ($\sim c$). Consequently, $L_{max}/\sqrt{k}$ is approximately inversely proportional to c for given values of M_2 and ε [equation (13)]. This trend is evident in Fig. 1. Furthermore, as expected, L_{max} decreases as the initial Mach number M_2 increases. At a Reynolds number of 1·0 (Fig. 2), the viscous and inertial resistances may be of approximately the same magnitude, and the latter plays a lesser role than in the results of Fig. 1. A further point to observe from Fig. 2 is the considerably reduced range of allowable values of M_2 consistent with $L_{max}/\sqrt{k} \geqslant 10$.

Finally, when the Reynolds number is as low as 0·1, the Darcy resistance predominates and c has only a minor effect in the calculation of $L_{max}/\sqrt{k}$. This is indicated in Fig. 3, where the curves are seen to group according to the values of the porosity. Again, the range of allowable values of M_2 is further reduced.

FLOW INTO THE POROUS MATERIAL

When the fluid enters the front face of the porous material, it experiences a sudden change in flow area. Emanuel and

Jones [3] discussed the importance of including this entrance effect in the complete analysis of the flow through the porous material. Numerical results for the M_1, M_2 relation are presented here.

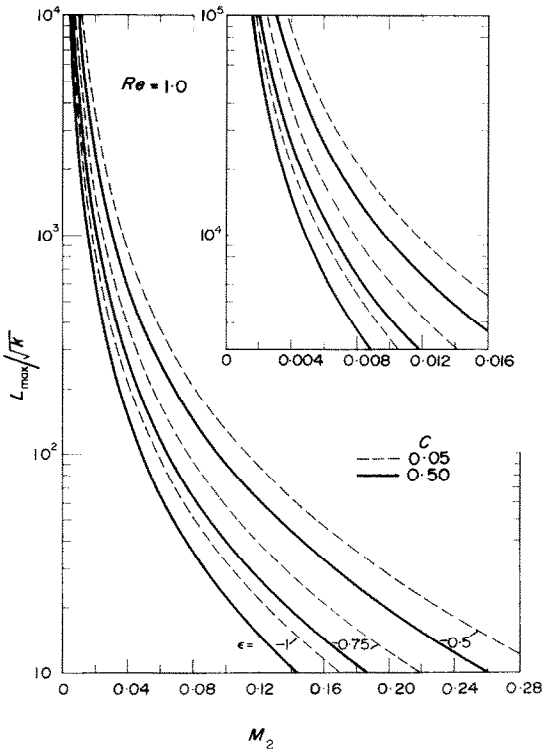

FIG. 2. Axial length of porous material for choking, $Re = 1{\cdot}0$.

In [3], it was assumed that the flow between stations 1 and 2 is analogous to that in a converging nozzle, with the flow undergoing an isentropic change. The Mach numbers at 1 and 2 are then related by the expression

$$\frac{\varepsilon^2 M_2^2}{M_1^2} = \left[\frac{1 + (\gamma - 1)M_2^2/2}{1 + (\gamma - 1)M_1^2/2}\right]^{(\gamma+1)/(\gamma-1)} \tag{15}$$

This relationship has been evaluated for several values of the porosity and the results are plotted in Fig. 4. This figure demonstrates that for intermediate and small porosities, M_1 may be appreciably less than M_2. This characteristic, taken together with the aforementioned limitations on M_2, may impose important restrictions on the allowable values of M_1.

ACKNOWLEDGEMENTS

This work arose out of research programs supported by the National Science Foundation under Grant GK–13303

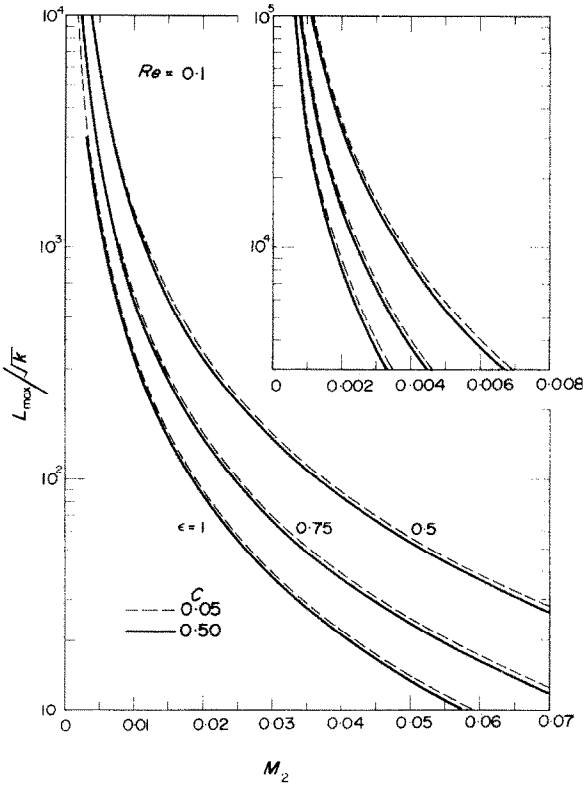

FIG. 3. Axial length of porous material for choking, $Re = 0{\cdot}1$.

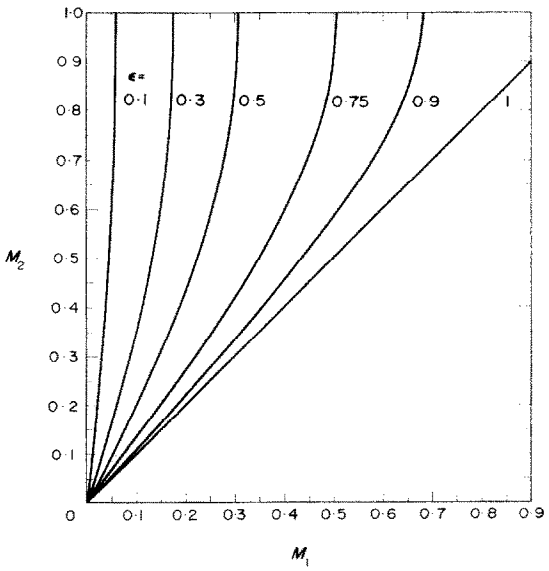

FIG. 4. Relationship between Mach numbers at the front face of the porous material.

and by the Department of Defence under Project THEMIS, NOOO14-68-A-0141-0001, administered by the Office of Naval Research. The support of these agencies is gratefully acknowledged.

REFERENCES

1. P. C. CARMAN, *Flow of Gases Through Porous Media*. Butterworths Scientific Publications, London (1956).
2. A. E. SCHEIDEGGER, *The Physics of Flow Through Porous Media*. Macmillan, New York (1960).
3. G. EMANUEL and J. P. JONES, Compressible flow through a porous plate, *Int. J. Heat Mass Transfer* **11**, 827–836 (1968).
4. J. SCHWARTZ and R. F. PROBSTEIN, Experimental study of slurry separators for use in desalination, *Desalination* **6**, 239–266 (1969).
5. G. S. BEAVERS and E. M. SPARROW, Non-Darcy flow through fibrous porous media, *J. Appl. Mech.* **36**, 711-714 (1969).
6. J. C. WARD, Turbulent flow in porous media, *J. Hydraulics Div. Proc. Am. Soc. Civil Engrs* **90**, HY5, 1–12 (1964).
7. A. H. SHAPIRO, *The Dynamics and Thermodynamics of Compressible Fluid Flow*, Vol. 1. The Ronald Press, New York (1953).
8. P. C. WANKAT and W. R. SCHOWALTER, Stability of combined heat and mass transfer in a porous medium, *Physics Fluids* **13**, 2418–2420 (1970).

Int. J. Heat Mass Transfer. Vol. 14, pp. 1859–1862. Pergamon Press 1971. Printed in Great Britain

AN IMPROVED TRANSFORMATION OF THE PATANKA – SPALDING TYPE FOR NUMERICAL SOLUTION OF TWO-DIMENSIONAL BOUNDARY LAYER FLOWS

V. E. DENNY and R. B. LANDIS

Department of Energy and Kinetics, School of Engineering and Applied Science, University of California, Los Angeles, California, U.S.A.

(*Received* 13 *January* 1971)

INTRODUCTION

SUBSTANTIAL impetus has been given to the numerical solution of two-dimensional boundary layer flows by the work of Patankar and Spalding [1, 2]. The primary contribution consists of a coordinate transformation (hereafter, the "ω-transformation") from the physical variables (x, y) to variables (x, ω), where

$$\omega = \int_0^y \rho u \mathrm{d}y / \int_0^{y_E} \rho u \mathrm{d}y = (\psi - \psi_I)/(\psi_E - \psi_I) \qquad (1)$$

and the subscripts I and E denote, respectively, the inner and outer edges of the boundary layer. Use of the non-dimensional stream function ω as the cross-stream variable confines the boundary layer to the rectangular region $x > 0$, $0 \leqslant \omega \leqslant 1$. This fact coupled with a working expression for mass entrainment, $\mathrm{d}\psi_E/\mathrm{d}x$, results in efficient utilization of the grid network in a finite difference solution.

The present authors have encountered some unexpectedly large errors in results obtained with this formulation, particularly when finite difference analogues of the governing differential equations are derived from Taylor series expansions. This is the result of inherent inaccuracies in finite difference approximations in the near wall region since

$$\partial u/\partial \omega = \frac{\partial u}{\partial y}\frac{\partial y}{\partial \omega} = \frac{\Delta \psi \partial u}{\rho u \partial y}, \qquad (2)$$

and all higher derivatives of u with respect to ω, become infinite as $y \to 0$. The resulting higher truncation errors at node points placed near the wall is of primary concern due to its effect on the extraction of wall gradients.

Patankar and Spalding circumvented this difficulty by matching a Couette flow analysis in the near wall region with the finite difference solution away from the wall. Although this is undoubtedly satisfactory for most applications, the complexity of the concept combined with the need to derive new expressions for each class of problems treated has resulted in rejection of this feature by many authors [3–5]. In addition, Patankar and Spalding recommend that difference analogues be obtained by integrally averaging the conservation equation over a control volume extending from $\omega_{i-\frac{1}{2}}$ to $\omega_{i+\frac{1}{2}}$ with an assumed linear variation of the dependent variable between adjacent node